

Thermoelectric Modeling of the Non-Ohmic Differential Conductance in a Tunnel Junction containing a Pinhole

Z.-S. Zhang and D.A. Rabson*

*Department of Physics, University of South Florida,
Tampa, FL 33620, USA*

To test the quality of a tunnel junction, one sometimes fits the bias-dependent differential conductance to a theoretical model, such as Simmons's formula. Recent experimental work by Åkerman and collaborators, however, has demonstrated that a good fit does not necessarily imply a good junction. Modeling the electrical and thermal properties of a tunnel junction containing a pinhole, we extract an effective barrier height and effective barrier width even when as much as 88% of the current flows through the pinhole short rather than tunneling. A good fit of differential conductance to a tunneling form therefore cannot rule out pinhole defects in normal-metal or magnetic tunnel junctions.

PACS numbers: 85.75.Dd, 85.30.Mn, 73.40.Gk

I. INTRODUCTION

With recent rapid progress toward incorporating tunnel junctions into practical devices, such as magnetic sensors and MRAM,^{1,2,3,4} it has become increasingly important to assure junction quality. Pinhole shorts through the insulating layer of a nominal tunnel junction constitute a possible failure mode. As early as the 1960s and 1970s, a set of criteria emerged, attributed to Rowell (who also credits Giaever),⁵ for determining whether a particular device was a good tunnel junction. Only a few apply when neither metal junction superconducts. One is the exponential dependence of the resistance on the thickness of the insulating layer over a series of devices with increasing thickness; however, a simple model shows that classical pinholes can mimic this signature of tunneling.⁶

Another, more commonly used, criterion is a non-Ohmic differential conductance.^{7,8} Simmons⁹ and Brinkman, Dynes, and Rowell¹⁰ calculated the tunneling current I through idealized junctions as functions of bias V , the height of the energy barrier, and the thickness of the insulator; when differential conductance dI/dV shows positive curvature, can be fit to one of these forms, and yields "reasonable" values for the barrier height and thickness, comparable to independent measurements, a good junction is sometimes presumed. Åkerman and collaborators have demonstrated experimentally that this criterion alone cannot establish the quality of a junction.^{11,12} They made a set of junctions with one normal and one superconducting lead. Above the superconducting-transition temperature, all fit the tunneling models well. Below the superconducting transition, in some of the junctions the current was suppressed inside the gap, as would be expected for tunneling from a normal metal through an intact insulator into a superconductor. Other junctions, however, instead showed the *enhancement* of current inside the gap typical of Andreev reflection, indicating essentially direct superconductor-metal contact.^{13,14}

We now demonstrate, in a simple model, how a tunnel junction with a pinhole short might reproduce the non-superconducting result, finding that as much as 88% of the current might flow through the short and still leave enough tunneling to give a good fit to the Simmons model.

A sample known to harbor a pinhole may show a differential conductance with either positive or negative curvature,¹⁵ the latter a heating effect: a pinhole will dissipate more heat at greater bias, becoming hotter, and, assuming it acts as a metal, conduct less. By contrast, the conductance of a tunneling channel increases with bias, as carriers see an effectively narrower trapezoidal barrier.^{16,17} The pinhole and the tunneling channels, therefore, have opposite effects on the curvature, the one tending to make the conductance curve down, the other making it curve upward. For parameters based on an experimental geometry, we find that the large positive curvature of a relatively small tunnel current can overwhelm the weakly negative curvature of the conductance through the pinhole short, still yielding an excellent fit to the Simmons form with apparent barrier width and height varying from the true width and height by factors of 2–3.

Although two of the Rowell criteria are found unreliable, the temperature dependence of conductance still appears to distinguish good junctions from shorted ones.^{11,12,18,19} Recently, we have proposed an additional test, using only electrical measurements at a single temperature, that may serve both to diagnose the presence of a pinhole and to determine its location.²⁰

II. MODEL AND COMPUTATION

We build a three-dimensional network, each node of which is defined by material, position, thickness, and length. The voltage and temperature at each node are computed iteratively, in turn determining the local electrical resistivity and thermal conductivity. We extract

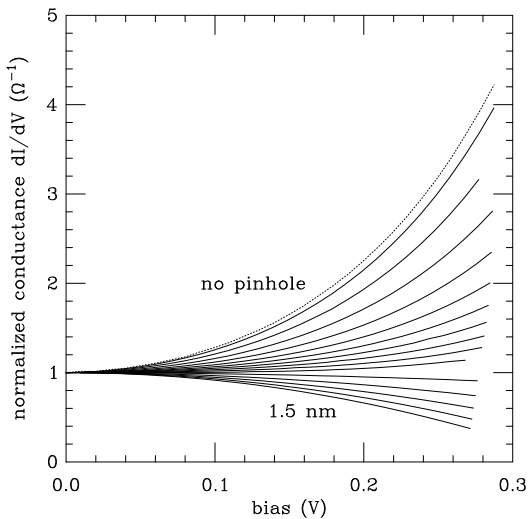


FIG. 1: Normalized differential conductance against bias. The dotted line plots differential conductance absent any pinhole; the solid lines trace conductance as the pinhole side changes (top to bottom) from 0.1 nm to 1.5 nm in increments of 0.1 nm. The separatrix between negative and positive curvature corresponds to a pinhole side between 1.0 nm and 1.1 nm. The bottom-layer temperature is 77K.

our dimensions from the experimental geometry in reference 11: the side of the tunnel junction is $50\mu\text{m}$; the bottom electrode is Nb of thickness 80 nm. On top of the Nb layer are an Al layer 8.5 nm thick and a 2.0 nm AlO_x barrier; then Fe (50 nm) is deposited on top. We set the barrier height at 0.5 eV. We model the pinhole as a metallic (Al) right square prism at the center of the tunnel junction. We alternate calculations of the voltage and the temperature at each node until reaching a steady state before measuring the effective resistance of the junction.

The electrical boundary conditions fix one edge of the bottom metallic layer at ground and one edge of the top metallic layer (rotated 90° relative to the grounded edge) at some positive voltage (the “input voltage”). The measured bias is the difference between the average voltages on the two edges opposite the fixed edges. (This simulates a four-terminal measurement of the sort we have previously modeled in Reference 20. The measured bias is generally somewhat smaller than the input voltage.) We hold the bottom metallic layer in equilibrium with a fixed heat bath; all heat generated in the junction must leave through this surface. All other surfaces are assumed perfect thermal insulators. (Radiation losses are ignored.)

There are several approaches to non-linear electro-thermal modeling.^{21,22} Here, we alternate relaxation methods for the voltage and the temperature at each node. The total electrical current through each node is

zero (Kirchhoff’s law), so that for a node A ,

$$\sum_i \frac{(V_A - V_i)}{R_{Ai}} = 0 \quad , \quad (1)$$

where V_j is the voltage at node j ($= A, i$) and the sum runs over the nearest neighbors of A . The resistance R_{Ai} between nodes A and i depends on the average of the temperatures T_A and T_i of the two nodes and, in the case of the tunneling layer, on the voltage difference $V_A - V_i$ through Simmons’s formula.^{9,23} Equation (1) is set as a large sparse matrix and solved with the standard SLATEC package. Similarly, the total heat flux through a node is equal to the heat generated Ohmically:

$$\sum_i \frac{(T_A - T_i) K_i (\frac{1}{2}(T_A + T_i))}{X_{Ai}} = \sum_i \frac{(V_A - V_i)^2}{(S_{Ai} R_{Ai})} \quad , \quad (2)$$

where K_i is the temperature-dependent thermal conductivity corresponding to the material of node i , X_{Ai} is the distance between nodes A and i , and S_{Ai} is the cross-sectional area spanned by the link between the nodes. First, (1) is solved; it must be iterated until voltages (checked at the pinhole and away from the pinhole) converge, since R_{Ai} through the insulating layer depends on the voltage drop. Then the temperature at each node is determined through (2), and the procedure is repeated until voltages and temperatures both converge.

III. RESULTS

We consider runs with the bottom layer held at 77K and with the side of the pinhole ranging from 0.1 nm to 1.5 nm. For an input voltage of 0.3V, we find the

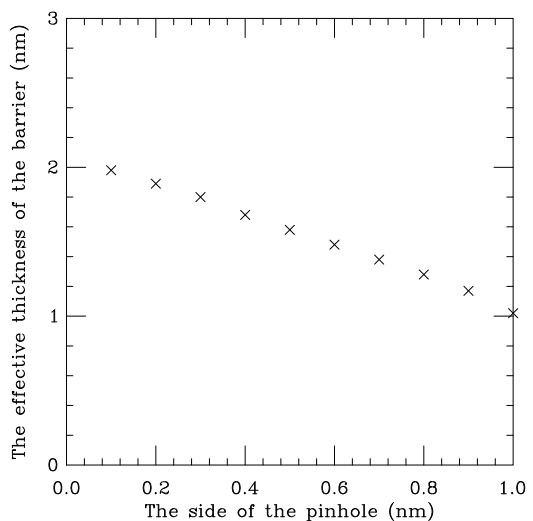


FIG. 2: The effective thickness of the barrier against the side of the pinhole. The true barrier thickness is 2.0 nm. The bottom-layer temperature is 77K.

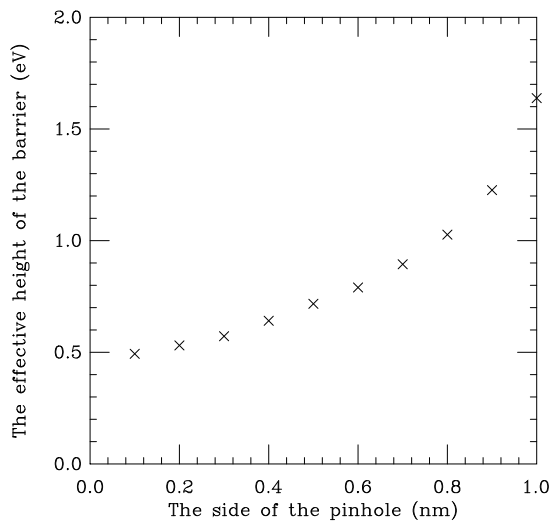


FIG. 3: The effective height of the barrier against the side of the pinhole. The true barrier height is 0.5 eV. The temperature is 77K.

maximum steady-state temperature at the center of the pinhole for the largest pinhole to be 86K. This rise of 9K is comparable to that estimated in Reference 15. The temperature rise rapidly falls off away from the pinhole.

As illustrated in Figure 1, the differential conductance may show positive or negative curvature, depending on pinhole size; we graph normalized curves for the pinhole side ranging from 0.1 nm to 1.5 nm, with the separatrix between 1.0 nm and 1.1 nm. When its curvature is positive, we can fit dI/dV to Simmons's formula to extract

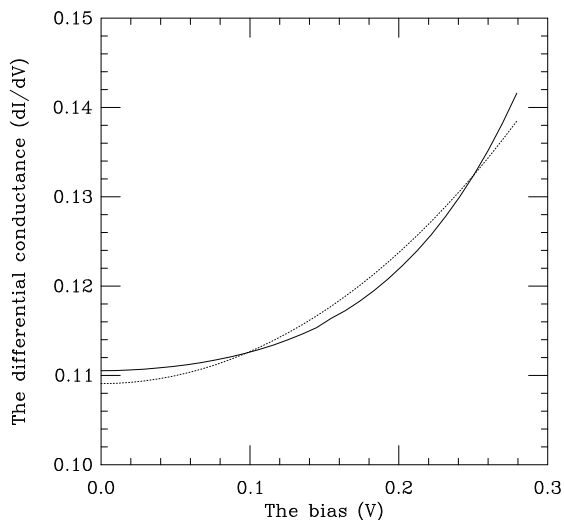


FIG. 4: Even in the presence of a large pinhole (0.9 nm on a side), the curvature of differential conductance can be fit to the form of Simmons. The solid line plots the simulation, while the dotted line plots Simmons's formula for the best-fit barrier height and thickness. The bottom-layer temperature is 77K.

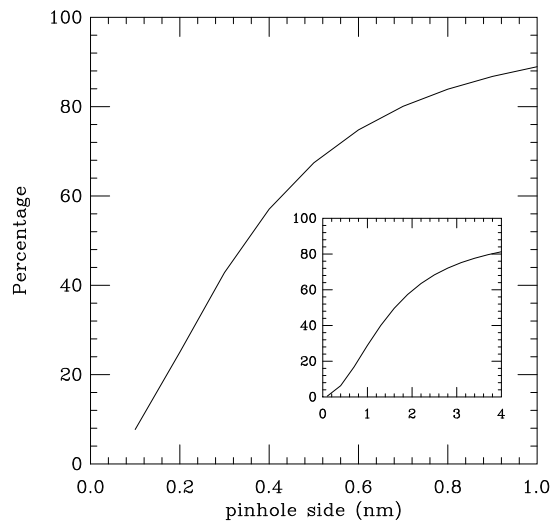


FIG. 5: The percentage of current that flows through the pinhole against the side of the pinhole with the bottom layer held at 77K (main graph) and 300K (inset). The input voltage is 0.3V.

an effective barrier thickness and effective height. These effective barrier parameters are shown in Figures 2 and 3. Without a pinhole, we recover essentially the input parameters. As the pinhole grows in size, the fits remain quite good (Figure 4), but the effective barrier parameters vary: the apparent barrier thickness decreases, while the apparent barrier height increases. The decreasing apparent thickness has the greatest effect on the overall conductance (which increases), while the increasing apparent height tends mostly to flatten the curve of differential conductance. Such trends are consistent with a simple WKB treatment of tunneling.¹⁷ We obtain similar results with the bottom layer held at 300K; the separatrix between positive and negative curvature occurs for a pinhole side between 4.0 nm and 4.1 nm.

From the above simulations, we obtain the percentage of the total current flowing through the pinhole (Figure 5). This percentage will increase with the side of the pinhole; the highest value corresponding to a positive curvature of dI/dV is 88% at 77K. (The highest value is 81% at 300K.)

Our simulations support the contention that a good fit of differential conductance to the Simmons form fails, by itself, to verify the quality of a tunnel junction.

Acknowledgments

We thank Johan Åkerman for useful discussions. DAR is a Cottrell Scholar of Research Corporation, which has funded part of this research. Numerical work was carried out at the Research-Oriented Computing Center of the University of South Florida.

-
- * Corresponding author
- ¹ S. S. P. Parkin, K. P. Roche, M. G. Samant, P. M. Rice, R. B. Beyers, R. E. Scheuerlein, E. J. O'Sullivan, S. L. Brown, J. Bucchigano, D. W. Abraham, et al., *J. Appl. Phys.* **85**, 5828 (1999).
- ² J. M. Daughton, A. V. Pohm, R. T. Fayfield, and C. H. Smith, *J. Phys. D : Appl. Phys.* **32**, R169 (1999).
- ³ W. Reohr, H. Hönigschmid, R. Robertazzi, D. Gogl, F. Pesavento, S. Lammers, K. Lewis, C. Arndt, Y. Lu, H. Viehmann, et al., *IEEE Circuits and Devices Magazine* (Sept.), 17 (2002).
- ⁴ M. Durlam, P. J. Naji, A. Omair, M. DeHerrera, J. Calder, J. M. Slaughter, B. N. Engel, N. D. Rizzo, G. Grynkewich, B. Butcher, et al., *IEEE Journal of Solid-State Circuits* **38**, 769 (2003).
- ⁵ J. M. Rowell, in *Tunneling Phenomena in Solids*, edited by E. Burstein and S. Lundqvist (Plenum, New York, 1969), p. 273.
- ⁶ D. A. Rabson, B. J. Jönsson-Åkerman, A. H. Romero, R. Escudero, C. Leighton, S. Kim, and I. K. Schuller, *J. Appl. Phys.* **89**, 2786 (2001).
- ⁷ J. S. Moodera and G. Mathon, *J. Magn. Magn. Mater.* **200**, 248 (1999).
- ⁸ J. Wang, P. P. Freitas, and E. Snoeck, *Appl. Phys. Lett.* **79**, 4553 (2001).
- ⁹ J. G. Simmons, *J. Appl. Phys.* **34**, 1793 (1963).
- ¹⁰ W. F. Brinkman, R. C. Dynes, and J. M. Rowell, *J. Appl. Phys.* **41**, 1915 (1970).
- ¹¹ B. J. Jönsson-Åkerman, R. Escudero, C. Leighton, S. Kim, I. K. Schuller, and D. A. Rabson, *Appl. Phys. Lett.* **77**, 1870 (2000).
- ¹² J. J. Åkerman, R. Escudero, C. Leighton, S. Kim, D. A. Rabson, R. W. Dave, J. M. Slaughter, and I. K. Schuller, *J. Magn. Magn. Mater.* **240**, 86 (2002).
- ¹³ G. E. Blonder, M. Tinkham, and T. Klapwijk, *Phys. Rev. B* **25**, 4515 (1982).
- ¹⁴ G. E. Blonder and M. Tinkham, *Phys. Rev. B* **27**, 112 (1983).
- ¹⁵ J. Schmalhorst, H. Brückl, M. Justus, A. Thomas, G. Reiss, M. Vieth, G. Gieres, and J. Wecker, *J. Appl. Phys.* **89**, 586 (2001).
- ¹⁶ C. B. Duke, *Tunneling in Solids*, vol. 10 of *Solid-State Physics* (Academic Press, New York, 1969).
- ¹⁷ E. Merzbacher, *Quantum Mechanics* (Wiley, New York, 1997).
- ¹⁸ J. J. Åkerman, J. M. Slaughter, R. W. Dave, and I. K. Schuller, *Appl. Phys. Lett.* **79**, 3104 (2001).
- ¹⁹ U. Rüdiger, R. Calarco, U. May, K. Samm, J. Hauch, H. Kittur, M. Sperlich, and G. Güntherodt, *J. Appl. Phys.* **89**, 7573 (2001).
- ²⁰ Z.-S. Zhang and D. A. Rabson (2003), preprint, URL cond-mat/0306153.
- ²¹ A. L. Palisoc and C. C. Lee, *J. Appl. Phys.* **64**, 6851 (1988).
- ²² D. Georg, L. Steffi, and K. Erich, *IEEE Transactions on very large scale integration (VLSI) systems* **5(3)**, 6515 (1997).
- ²³ Simmons gives dI/dV at zero temperature. We have incorporated heuristically an additional linear increase in the overall conductance with temperature following the data in Reference 11; a more detailed treatment would take as its starting point thermal smearing of the Fermi surface, as in J. J. Åkerman, I. V. Roschin, J. M. Slaughter, R. W. Dave, and I. K. Schuller, *Europhys. Lett.* **63**, 104 (2003).